



Influences of Aggregate Type and Morphology on the Mechanical Performance of Concrete

Fereshteh Rahmani¹, Alka Subedi¹, Sushmit Sharma Bhattarai¹, Hyunhwan Kim¹, Soon-Jae Lee¹
¹Texas State University

The performance of concrete is strongly influenced by the type, morphology, and proportion of coarse aggregates used in the concrete mixture. This study examines how combining limestone (LS) with siliceous river gravel (RG) and crushed river gravel (CRG) affects key properties of concrete, focusing on abrasion resistance, coefficient of thermal expansion (CTE), and dynamic modulus of elasticity. Six mixture designs were developed with varying aggregate ratios and were tested in accordance with ASTM and TxDOT standards. Results showed that mixtures containing CRG exhibited higher abrasion resistance, primarily due to greater angularity and surface texture that enhanced aggregate interlock. The CTE of CRG mixtures was 3–10% higher than that of RG mixtures, reflecting stronger mechanical bonding and greater thermal strain transfer. Increasing LS content reduced CTE, improving dimensional stability. Dynamic modulus results indicated that CRG mixtures achieved up to 4% higher stiffness. Overall, aggregate type and morphology significantly influence mechanical and thermal performance. Optimizing aggregate blending, particularly by incorporating angular CRG with LS, can improve stiffness, abrasion resistance, and thermal stability, enhance durability of concrete structure.

Keywords: Coarse aggregate type; Abrasion resistance; Coefficient of thermal expansion; Dynamic modulus; Limestone; River gravel.

Introduction

Concrete is the backbone material of modern infrastructure, forming the structural basis of highways, bridges, industrial floors, airfields, and other critical civil works. In these applications, long-term performance under sustained loading and environmental exposure is influential to ensure structural safety, serviceability, and cost efficiency. The mechanical and thermal behavior of concrete directly governs its resistance to cracking, deformation, and surface wear, all of which are influenced by the characteristics of its constituent materials. Among these, the selection and proportioning of coarse aggregates play a decisive role in determining the structural integrity and service life of concrete infrastructure, making aggregate optimization a key consideration in durable mixture design (Fookes, 1980). Coarse aggregates, comprising the large volume fraction in concrete (typically 60–80%), serve not only as inert fillers but also as contributors to stiffness, strength, wear resistance, and thermal

stability (McCullough & Saraf, 1989). Their mineral composition, surface texture, shape, and gradation directly affect performance parameters such as abrasion resistance, coefficient of thermal expansion (CTE), and elastic modulus (Basheer et al., 2005). In large-scale construction applications, particularly those exposed to heavy mechanical loads and significant temperature variations, these parameters collectively determine the concrete's ability to resist cracking, maintain dimensional stability, and preserve functional surface conditions throughout its service life. Across many regions of the United States, coarse aggregates such as limestone (LS) and siliceous river gravel (RG) are widely utilized in concrete production, selected based on local availability, cost, and performance requirements. Uncrushed river gravel (RG) consists of naturally rounded particles with relatively smoother surfaces, whereas crushed river gravel (CRG) is produced by mechanically crushing river gravel, creating more angular particles with fractured faces and increased surface roughness. Limestone, primarily composed of calcium carbonate, offers advantages in terms of workability and strong bonding with cement paste but exhibits relatively low hardness and abrasion resistance. In contrast, siliceous river gravel, rich in quartz and silicate minerals, provides superior hardness and wear resistance but is often rounded and polish-prone, leading to reduced surface friction over time (Yang et al., 2023). Furthermore, the higher thermal expansion potential of RG can induce internal stresses during temperature fluctuations, promoting curling, cracking, and premature deterioration when aggregate thermal compatibility is not adequately managed (Howlader et al., 2012). If aggregate thermal compatibility is not properly managed, these effects can increase the risk of premature pavement deterioration (Sabih & Tarefder, 2020; Subedi et al., 2025). Crushing river gravel alters its morphology, enhancing angularity and surface texture, thereby improving mechanical interlock, bond strength, and resistance to polishing (Hong et al., 2014). However, the thermal behavior of such crushed aggregates and their interaction with limestone in blended systems remains an area requiring further study to optimize concrete mixture designs for infrastructure-scale applications. This study investigates the influence of blending limestone with both crushed and uncrushed river gravel on key performance parameters relevant to construction applications. Through a systematic laboratory program, six concrete mixtures were evaluated for abrasion resistance, CTE, and dynamic modulus of elasticity. These parameters collectively define surface durability, dimensional stability, and stiffness as key indicators of long-term performance in structural concrete. The outcomes of this research aim to support performance-based aggregate selection and mixture optimization strategies that enhance durability, minimize maintenance requirements, and extend the service life of concrete infrastructure across varying climatic and loading conditions.

Methodology

The systematic laboratory experimental approach was used to investigate the influence of coarse aggregate properties on three critical concrete performance parameters: abrasion resistance, CTE and dynamic modulus of elasticity. In this study, two sets of concrete specimens were prepared to evaluate the abrasion resistance of concrete using different coarse aggregate types (i) limestone combined with regular river gravel (ii) limestone combined with crushed river gravel. Across all mixtures, cement content and batch volume were held constant. Water and sand contents were adjusted slightly to account for absorption differences while keeping the primary variable as the coarse aggregate replacement level; admixture dosage was kept constant. The proportion of coarse aggregates in each mixture design is summarized in Table 1. The gradation of the crushed river gravel was selected based on ASTM C33 gradation for coarse aggregate (Texas Department of Transportation, 2014). All concrete mixtures were

proportioned using Type I/II Portland cement with no supplementary cementitious materials and natural river sand as fine aggregate. A constant water-to-cementitious materials ratio (w/cm) of 0.35 was maintained for all mixtures. The target slump was 4–6 inches (100–150 mm), and no air-entraining admixture was used, resulting in 0% air content. These parameters were kept consistent across all mixtures to isolate the effect of coarse aggregate type on concrete performance. Coarse aggregate morphology (e.g., angularity and surface texture) was treated as a categorical variable based on the aggregate source and processing route: natural river gravel (uncrushed), crushed river gravel (mechanically crushed), and crushed limestone. Morphological descriptors (rounded vs. angular; smoother vs. rougher surface) are used in a qualitative sense based on visual inspection of representative particles prior to batching. A dedicated instrument-based angularity test (e.g., AIMS/laser profilometry) and a fractured-face percentage test were not performed in this study.

Table 1. The proportion of coarse aggregates in each mixture design

Mixture ID	Limestone (LS) (%)	(i)	(ii)
		River Gravel (RG) (%)	Crushed River Gravel (CRG) (%)
Mixture 1 (100% RG)	0	100	100
Mixture 2 (80% RG, 20% LS)	20	80	80
Mixture 3 (60% RG, 40% LS)	40	60	60
Mixture 4 (40% RG, 60% LS)	60	40	40
Mixture 5 (20% RG, 80% LS)	80	20	20
Mixture 6 (100% LS)	100	0	0

For each mixture, five concrete samples were cast in a cylindrical mold of size 4" x 8" (approximately 100 mm x 200 mm) and cured for 28 days. After curing, the specimens were subjected to the following testing procedures.

Abrasion resistance

The abrasion resistance of these specimens was evaluated using ASTM C944. Each specimen was oven-dried at 77°F (25°C) prior to testing. The test was conducted on both the top and bottom surfaces of each cylindrical concrete specimen. A rotating abrasion cutter was applied to the surface under a constant load of 98 N, spinning at 150 revolutions per minute. Each surface underwent three abrasion cycles, with each cycle lasting 160 seconds. After each cycle, the apparatus was turned off, and the specimen was removed and cleaned using a soft brush or air blower to eliminate any loose abraded material. The initial and final weights of the specimens were recorded using a digital scale with a precision of 0.01 grams, and the total weight loss was calculated as a measure of abrasion resistance.

Coefficient of thermal expansion (CTE)

CTE testing was carried out following the TxDOT Designation: Tex-428-A standard (Texas Department of Transportation, 2023). For each mixture three samples were used to carry out the CTE testing. Concrete cylinder specimens, each measuring 175–180 mm in length according to the test configuration, were prepared and properly conditioned by soaking them in lime water for 48 hrs. prior to the testing to ensure uniform moisture content and temperature equilibrium before testing. With a focus on

measuring the CTE of hydraulic cement concrete in compliance with AASHTO T336 and minimizing operator interaction, the System equipped with displacement transducer and a temperature-controlled water bath was used to measure CTE. During the test specimens were subjected to a controlled thermal cycle, typically ranging from 10°C to 50°C. The displacement transducer tracks length changes of the specimen during temperature variation. The system ensures consistency by applying a tolerance of 0.3×10^{-6} mm/mm/°C between segments. Data collected included temperature versus change in length, with CTE values reported in both imperial (in/in/°F) and SI (mm/mm/°C) units.



Figure 1. Equipment frame settings for CTE Measurement

Dynamic modulus of elasticity

Dynamic modulus of elasticity of the concrete samples was measured using Concrete Resonant Frequency device, known as the Emodumeter which meets Standard Test Method for Fundamental Transverse, Longitudinal, and Torsional Resonant Frequencies of Concrete Specimens (ASTM International, 2019b). The concrete samples were placed in the supported bench fixture; impact is caused by hitting the center of the specimen with hardened steel balls. The system detects vibrations caused by a hardened steel ball impact, which were measured by an accelerometer and analyzed by the Emodumeter to produce a frequency spectrum. The dynamic modulus of elasticity, E , in pascals, was determined using the fundamental longitudinal resonant frequency obtained from the impact resonance method:

$$E = D \times M \times f_{ln}^2$$

where M is specimen mass (kg), f_{ln} is the fundamental longitudinal resonant frequency (Hz), and D is a geometry-dependent coefficient determined by the specimen's length and diameter.



Figure 2. Emodumeter setup for Young's Modulus of Elasticity measurement

Results and Discussion

Abrasion resistance test: surface mass loss trends

Graphs in figure 3, present the average mass loss recorded on the top and bottom surfaces of specimens prepared with different combinations of LS, RG, and CRG. Six mixtures were evaluated, ranging from 100% RG or CRG to 100% LS. The results compare the surface wear performance of the limestone–river gravel with that of the limestone–crushed river gravel aggregate combination.

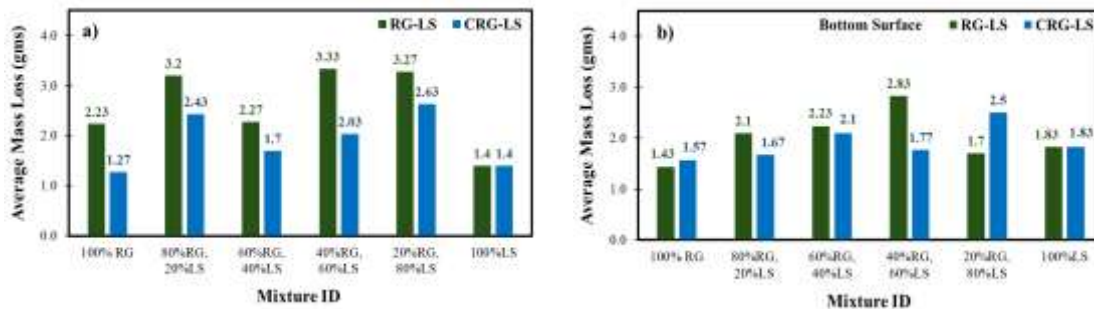


Figure 3. Average mass loss comparison between different mixtures for a) top surface and b) bottom surface of concrete specimens.

Across all mixtures, the LS&CRG combinations exhibited generally lower average weight losses than the corresponding LS&RG mixtures, particularly on the top surface. The reduction in top-surface wear for the LS&CRG mixtures averaged approximately 0.7 g compared with LS&RG. This improvement is attributed to the angularity and rough surface texture of crushed aggregates, which promote better interlocking and enhance abrasion resistance. For the top surfaces, the LS&RG system showed the highest weight losses in Mixture 4 (3.33 g) and Mixture 5 (3.27 g) which can be related to the less abrasion resistance properties of Limestone, whereas the lowest was observed in Mixture 6 (1.40 g i.e. 100% LS) that might support crushed limestone aggregates has angular, rough surfaces that bond well with the cement paste, producing a strong interfacial transition zone. In contrast, the LS&CRG mixtures consistently displayed reduced wear, with Mixture 4 decreasing from 3.33 g (LS&RG) to 2.03 g (LS&CRG). These results indicate that the incorporation of crushed gravel effectively mitigates surface degradation under the same test conditions. The bottom-surface weight losses followed a less consistent pattern. Although LS&CRG generally resulted in lower or comparable bottom-surface wear (e.g., Mixture 2: 2.10 → 1.67 g; Mixture 4: 2.83 → 1.77 g), certain mixtures such as Mixture 5 exhibited slightly higher losses (1.70 → 2.50 g). The contributing factors for higher bottom abrasion may be segregation and gradation issues and problems with compaction or curing. If we compare the overall performance, the LS&CRG specimens outperformed the LS&RG specimens in four of the six mixtures (Mixtures 1–4). Mixture 5 showed a mixture performance. The most significant improvement occurred in Mixture 4, where both top and bottom wear were substantially reduced in the LS&CRG configuration. Conversely, the LS&RG system showed greater total weight loss in blends containing higher proportions of river gravel, reflecting the smoother texture and lower mechanical interlock of rounded aggregates.

Coefficient of thermal expansion test

Figure 4 presents the average CTE values for concrete mixtures with different combinations of LS, RG, and CRG. The measured CTE values for CRG mixtures ranged from 4.20×10^{-6} to 5.02×10^{-6} in/in/°F, while those for the corresponding RG mixtures ranged from 3.71×10^{-6} to 4.65×10^{-6} in/in/°F. A consistent reduction in CTE was observed with increasing limestone content for both mixture types. The mixture containing 100% CRG (Mixture 1) exhibited the highest CTE, whereas the mixture containing 100% limestone (Mixture 6) showed the lowest value.

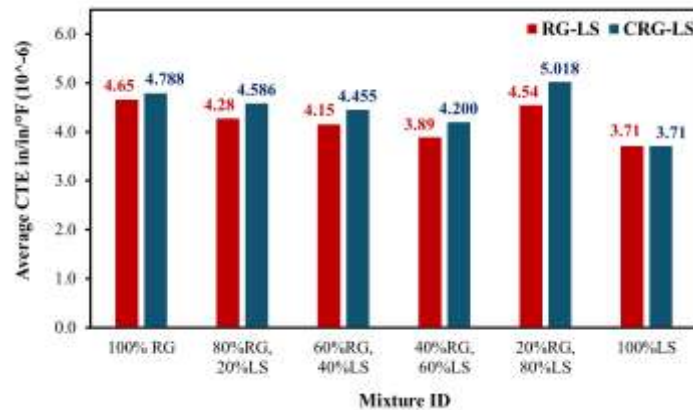


Figure 4. Average value of Coefficient of Thermal Expansion per mixture for different mixture composition

The CTE values for concrete mixture with CRG were approximately 3–10% higher than those containing RG, with an overall average increase of about 7% across all mixtures. This variation reflects the influence of aggregate morphology and interfacial properties. The angular and rough-textured nature of CRG promotes a stronger mechanical bond with the cement paste (An et al., 2017), which might lead to greater transfer of thermal strains and a higher overall CTE. In contrast, the smoother and rounded RG particles allow limited interfacial movement under temperature fluctuations, producing a comparatively lower expansion. The trend indicates that aggregate type and limestone replacement ratio strongly govern the thermal expansion characteristics of concrete. Increasing the limestone fraction progressively reduces the composite CTE, suggesting improved dimensional stability.

Dynamic modulus of elasticity results

The Dynamic Elastic Modulus Test, conducted as per ASTM C215-19, measured the resonant frequencies of cylindrical concrete specimens to assess stiffness and internal integrity non-destructively. Each of the six mixture designs was tested using three replicates (18 total), showing minimal variation ($COV \leq 1\%$). Using longitudinal vibration mode, the modulus was calculated from specimen geometry, mass, and frequency. As shown in Figure 5, results were influenced by the type and proportion of coarse aggregates used.

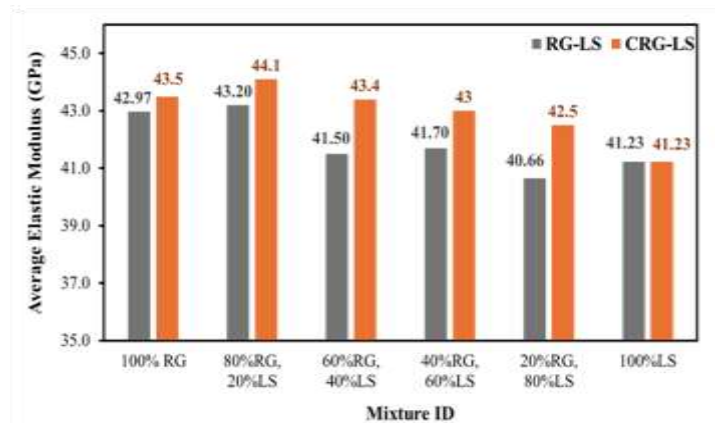


Figure 5. Average values of dynamic elastic modulus per mixture for different mixture composition

Figure 5 presents the average dynamic elastic modulus values for concrete mixtures containing different combinations of limestone (LS), river gravel (RG), and crushed river gravel (CRG). The measured modulus values for CRG mixtures ranged from 41.23 GPa to 43.50 GPa, while those for corresponding RG mixtures ranged from 41.50 GPa to 43.20 GPa. Across all comparable mixtures, the concrete mixtures with CRG exhibited dynamic modulus values approximately 0.5–4% higher than those containing RG, with an overall average increase of around 2.1%. The highest dynamic modulus (44.1 GPa) was recorded for Mixture 2 containing 80% CRG and 20% limestone, indicating an optimal blend that balances stiffness and aggregate interlocking. CRG, being angular and rough-textured, promotes improved mechanical interlocking and more efficient load transfer across the aggregate–paste interface. Additionally, as the proportion of limestone increased, a progressive decrease in dynamic modulus was observed, highlighting the impact of limestone's lower elastic modulus due to its predominantly calcite-based composition (Beyene et al., 2023). These findings indicate that aggregate characteristics, including type, surface texture, and angularity, influence the dynamic elastic modulus of concrete, alongside the stiffness contribution of the matrix.

Conclusion

This study evaluated the effects of coarse aggregate type, texture, and blending proportion on the performance parameters of concrete used in infrastructure construction, specifically abrasion resistance, CTE, and dynamic elastic modulus. The results highlight the role of aggregate characteristics in governing both mechanical and thermal behavior of structural concrete, which directly affects durability and performance under varying environmental and loading conditions.

- Concrete mixtures incorporating crushed river gravel (CRG) exhibited superior abrasion resistance compared to those containing rounded river gravel (RG), particularly on exposed surfaces. The angular and rough texture of CRG enhanced particle interlock and surface integrity, reducing wear loss under simulated mechanical wear. Conversely, mixtures with higher proportions of RG experienced greater surface abrasion, particularly when combined with softer limestone, due to reduced interfacial bonding and lower hardness.

- Concrete mixtures containing CRG displayed CTE values approximately 3–10% higher than those with RG, with an overall average increase of about 7%. The stronger aggregate–paste bond associated with angular CRG facilitated greater strain transfer during thermal cycling. Increasing the limestone content in blended systems consistently reduced CTE, indicating improved dimensional stability, an essential factor for minimizing thermally induced cracking and stress development in large-scale concrete structures.
- Concrete incorporating CRG achieved higher stiffness, with dynamic modulus values up to 4% greater than comparable RG mixtures. Mixtures with higher limestone content exhibited slightly lower moduli, consistent with the lower intrinsic stiffness of limestone, though this effect was mitigated by CRG’s angularity and surface roughness.

The findings demonstrate that aggregate morphology, mineralogy, and blending ratios influence concrete’s mechanical and thermal performance. Mixtures containing angular CRG and limestone provided enhanced stiffness, abrasion resistance, and thermal stability, offering advantages for concrete infrastructure exposed to mechanical wear and temperature fluctuations. In contrast, high proportions of rounded RG led to reduced mechanical interlock, greater wear, and higher susceptibility to thermal cracking. These results underscore the importance of performance-based aggregate selection and proportioning in concrete mix design to ensure durable, and resilient infrastructure systems across diverse construction environments. As limitations to be considered, this study was conducted under controlled laboratory conditions using a limited number of aggregate sources, which may restrict the direct generalization of results to all geological regions and material supplies. Aggregate morphology (angularity and surface texture) was characterized qualitatively based on visual inspection and processing history; no quantitative image-based analysis or fractured-face percentage testing was performed. All mixtures were produced with a constant water-to-cementitious materials ratio of 0.35 and without supplementary cementitious materials, limiting assessment of interactions between aggregate type and mixture chemistry. In addition, testing was performed at 28 days and does not capture long-term aging, moisture cycling, or field exposure effects. Therefore, while the results clearly demonstrate trends related to aggregate type and morphology, further research incorporating additional aggregate sources, quantitative shape analysis, varied mixture designs, and long-term durability testing is recommended.

References

Alfonso, D., Dugarte, M., Carrillo, J., & Arteta, C. (2024). Effect of aggregate type on the elastic modulus and compressive behavior of concrete: A case study in Colombia. *Construction and building materials*, *411*, 134131.

An, J., Kim, S., Nam, B., & Durham, S. (2017). Effect of Aggregate Mineralogy and Concrete Microstructure on Thermal Expansion and Strength Properties of Concrete. *Applied Sciences*, *7*(12), 1307. <https://doi.org/10.3390/app7121307>

ASTM International. (2019a). Standard Test Method for Abrasion Resistance of Concrete or Mortar Surfaces by the Rotating-Cutter Method. *ASTM C944/C944M-19*. https://doi.org/10.1520/C0944_C0944M-19

ASTM International. (2019b). Standard Test Method for Fundamental Transverse, Longitudinal, and Torsional Resonant Frequencies of Concrete Specimens. *ASTM C215-19*.

<https://doi.org/10.1520/C0215-19>

Beyene, M., Meiningner, R., & Munoz, J. F. (2023). Mineralogic and petrographic evaluation of aggregate quality—effect on compressive strength of concrete pavement. *International Journal of Pavement Engineering*, 24(2), 2088756.

Chen, Q., Zhang, J., Wang, Z., Zhao, T., & Wang, Z. (2024). A review of the interfacial transition zones in concrete: Identification, physical characteristics, and mechanical properties. *Engineering Fracture Mechanics*, 109979.

Cramer, S. M., & Carpenter, A. J. (1999). Influence of total aggregate gradation on freeze-thaw durability and other performance measures of paving concrete. *Transportation research record*, 1668(1), 1-8.

Delatte, N. (2018). *Concrete pavement design, construction, and performance*. Crc Press.

Fookes, P. (1980). An introduction to the influence of natural aggregates on the performance and durability of concrete. *Quarterly Journal of Engineering Geology and Hydrogeology*, 13(4), 207-229.

Fowler, D. W., & Rached, M. M. (2012). Polish resistance of fine aggregates in portland cement concrete pavements. *Transportation Research Record*, 2267(1), 29-36.

Hall, J. W., Smith, K. L., & Littleton, P. C. (2009). *Texturing of concrete pavements* (Vol. 634). Transportation Research Board.

Joumbat, R., Al Basiouni Al Masri, Z., Al Khateeb, G., Elkordi, A., El Tallis, A. R., & Absi, J. (2023). State-of-the-art review on permanent deformation characterization of asphalt concrete pavements. *Sustainability*, 15(2), 1166.

Lees, G., & Kennedy, C. K. (1975). Quality, shape, and degradation of aggregates. *Quarterly Journal of Engineering Geology*, 8(3), 193-209.

Liu, J., Mukhopadhyay, A. K., Celaya, M., Nazarian, S., & Zollinger, D. G. (2009). *Best practices for the use of siliceous river gravel in concrete paving*.

Lukefahr, E., & Du, L. (2010). Coefficients of Thermal Expansion of Concrete with Different Coarse Aggregates—Texas Data. *Journal of Testing and Evaluation*, 38(6), 683-690.

Mallela, J., Abbas, A., Harman, T., Rao, C., Liu, R., & Darter, M. I. (2005). Measurement and Significance of the Coefficient of Thermal Expansion of Concrete in Rigid Pavement Design. *Transportation Research Record*, 1919(1), 38-46. <https://doi.org/10.1177/0361198105191900105>

Naik, T. R., Kraus, R. N., & Kumar, R. (2011). Influence of types of coarse aggregates on the coefficient of thermal expansion of concrete. *Journal of Materials in Civil Engineering*, 23(4), 467-472.

Omoding, N., Cunningham, L. S., & Lane-Serff, G. F. (2021). Influence of coarse aggregate parameters and mechanical properties on the abrasion resistance of concrete in hydraulic structures. *Journal of Materials in Civil Engineering*, 33(9), 04021244.

Roshan, A., & Abdelrahman, M. (2024). Influence of aggregate properties on skid resistance of pavement surface treatments. *Coatings*, 14(8), 1037.

Sabih, G., & Tarefder, R. A. (2020). Predicting Long-Term Coefficient of Thermal Expansion of Paving Concrete. *Transportation Research Record*, 2674(9), 792-798.

Subedi, A., Kim, H., Lee, S.-J., & Lee, M.-S. (2025). Assessing Abrasion Resistance in Concrete Pavements: A Review. *Applied Sciences*, 15(4), 2101.

Suh, Y.-C., Jung, D.-H., & Park, K.-W. (2021). Comparison of CRCP and JCP based on a 30-year performance history. *International Journal of Pavement Engineering*, 22(13), 1651-1658.

Tarrer, A. (1991). The effect of the physical and chemical characteristics of the aggregate on bonding. Texas Department of Transportation. (2014). Hydraulic Cement Concrete. *TxDOT Specification Item 421*. <https://ftp.txdot.gov/pub/txdot-info/cmd/cserve/specs/2014/standard/s421.pdf>

Texas Department of Transportation. (2023). Test Procedure for Determining the Coefficient of Thermal Expansion of Concrete. *TxDOT Designation: Tex-428-A*. <https://www.txdot.gov/inside-txdot/division/materials/materials-manual.html>

Sabih, G., & Tarefder, R. A. (2020). Predicting long-term coefficient of thermal expansion of paving concrete. *Transportation research record*, 2674(9), 792-798.

Subedi, A., Kim, H., Lee, M.-S., & Lee, S.-J. (2025). Thermal Behavior of Concrete: Understanding the Influence of Coefficient of Thermal Expansion of Concrete on Rigid Pavements. *Applied Sciences* (2076-3417), 15(6).